A Novel Three-Pulse Equivalent Power Loss Profile for Simplified Thermal Estimation

Zhang, Yichi; Ge, Xinglai; Zhang, Yi; Xie, Dong; Bo, Yao; Wang, Huimin

Published in:
IEEE Journal of Emerging and Selected Topics in Power Electronics

DOI (link to publication from Publisher):
10.1109/JESTPE.2021.3070994

Publication date:
2021

Document Version
Accepted author manuscript, peer reviewed version

A Novel Three-Pulse Equivalent Power Loss Profile for Simplified Thermal Estimation

Yichi Zhang, *Student Member*, *IEEE*, Xinglai Ge, *Member*, *IEEE*, Yi Zhang, *Member*, *IEEE*, Dong Xie, *Student Member*, *IEEE*, Bo Yao, *Student Member*, *IEEE*, and Huimin Wang, *Student Member*, *IEEE*

***Abstract*- One of the key challenges for long-term reliability analysis of power electronic converters is to quickly estimate extensive junction temperature cycles of power semiconductor devices while fulfilling an accepted accuracy. To address this challenge, this paper proposes a novel three-pulse equivalent power loss profile. By contrast to the conventional methods of dividing the power loss equally, this paper discretizes the power loss profile based on the identified occurrences of maximum and minimum junction temperatures (i.e., thermal Characteristics). This proposed model decouples the conventional conflict between the thermal estimation accuracy and computational burdens. And it has the advantages of improving accuracy in terms of the maximum and minimum junction temperatures, and power-on time of thermal profiles, which are majorly concerned by today's lifetime models of power semiconductors. Moreover, the proposed method also helps to reduce computational burdens. The relevant variables of the thermal modeling methods are investigated. Finally, the effectiveness of the proposed method is verified through simulation and experiments, and the impact of its thermal estimation advantages on lifetime evaluation is analyzed further.**

***Index Terms*- Error analysis, equivalent power loss profile, junction temperature estimation, power semiconductor devices, thermal characteristics**

I. Introduction

With increasingly pursuing higher efficiency and power density in power electronics, reliability has been becoming one of the major bottlenecks in this industry [1], [2], in particular of the high failure rate of power semiconductor devices [3]. To achieve a better performance, reliability evaluation has played an essential role in designs, manufacturing, and operation of today's power electronics [4], such as to reduce design margins [5], to plan maintenance schedules [6], [7] etc.

Thermal stresses are one of the most critical factors for the reliability of power semiconductor devices, especially mean junction temperatures and temperature swings. According to [8] and [9], every 10 K increase of the mean junction temperature or 5 K increase of the temperature swing can reduce the lifetime of power semiconductor devices to half. As a result, reliability evaluation essentially relies on the electro-thermal analysis which converts the mission profiles into junction temperatures [10], [11].

Thermal behaviors of power semiconductor devices are classified into two categories: periodic and non-periodic power loss profiles, respectively [12], [13]. Among them, the periodic power loss profiles are caused by the varied fundamental-frequency currents and involve intensive computational burdens for thermal modeling. Firstly, the large amount of these thermal cycles accumulates non-negligible fatigues for power devices in many applications, especially for high-power and/or varied-frequency applications [14], [15]. Although the reliability impact of such temperature fluctuations in low-power applications is not obvious, intuitive ignorance of their effects is questionable under varied conditions. Besides, driven by continuous reduction of cost and safety margins in power electronics, the accuracy of thermal estimation under periodic power loss profile is increasing of significance for the reliability evaluation. However, a large amount of such temperature cycles (e.g., one-year mission profiles) causes highly computational burdens [16], and has not been fully solved. This challenge, thus, calls for a simplified thermal model that can quickly estimate the intensive junction temperature cycles while maintaining a specific accuracy.

In the existing junction temperature estimation, applying the convolution of the instantaneous power losses and the thermal impedance is a straightforward solution [17]. However, due to the time-varying power losses, for instance, the half-sine loss profile [18], [19], the convolution algorithm causes tremendous computational burdens, especially for long-term estimation. Equivalent discretization of power loss profiles is a commonly accepted solution to reduce computational burdens [20]-[22]. In the state-of-the-art, the power losses are equivalent to a square-wave loss profile in [20]. By doing so, the involved computational burden is greatly reduced but the estimation error can be up to 51.4% [20]. Following, a two-level equivalent loss profile is proposed to achieve a better junction temperature estimation in [21]. Comparing these two existing methods, it can be seen that the accuracy and computational complexity are compromised each other. With

This work was supported by the Project Supported by High-Speed Railway Joint Funds of the National Natural Science Foundation of China (U1934204) and the Project Supported by National Natural Science Foundation of China (51677156). (*Corresponding author: Xinglai Ge, Yi Zhang*).

Y. Zhang, X. Ge, D. Xie, and H. Wang are with the Ministry of Education Key Laboratory of Magnetic Suspension Technology and Maglev Vehicle, Southwest Jiaotong University, Chengdu 610031, China (e-mail: yichizhang@my.swjtu.edu.cn; xlgee@163.com; xiedong@my.swjtu.edu.cn; wanghuimin@my.swjtu.edu.cn).

Y. Zhang and B. Yao are with the Department of Energy Technology, Aalborg University, Aalborg 9220, Denmark (e-mail: yiz@et.aau.dk; ybo@et.aau.dk).

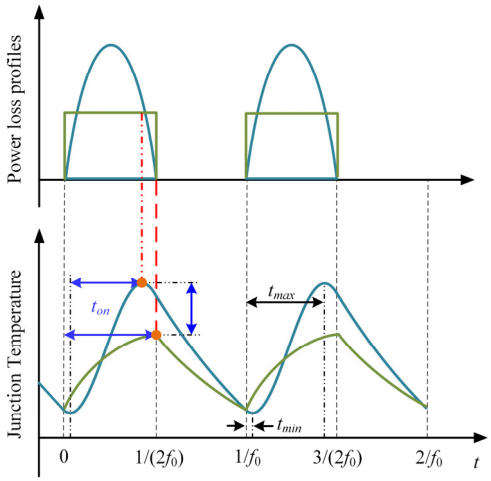

Fig. 1. Comparison of thermal behavior under actual power loss profile and square-wave equivalence, where t_{on} is the power on time, t_{max}, t_{min} are the exact occurrences of the maximum and the minimum junction temperatures.

this consideration, a generic simplification method is proposed in [22]. In this study, the relationship between the estimated error and computational burden is quantified through an analytical model. A minimum discretization level (i.e., the minimum number of power dissipation pules) can be obtained according to the maximum allowable error.

All the aforementioned methods provide much feasibility for simplified estimation of junction temperature, however, there are still some limitations, which mainly involves two aspects. On the one hand the power loss is divided equally, in which thermal estimation accuracy and computational burdens completely contradictory. In other words, the conventional methods improve accuracy at the cost of increasing the discrete power-loss pulses (i.e., increased computations). On the other hands, the existing methods further assume that the maximum temperature occurs at the end time of the maximum power loss. But this assumption often contradicts the practical thermo-physics. For example, as shown in Fig. 1, the maximum temperature is conventionally assumed to reach at t=1/(2f_0) for square-wave equivalence. However, the maximum junction temperature does not occur at the same time when the maximum equivalent power loss profiles end in practice.

The main reason for these limitations is that the original power loss profile is nonlinear, and the thermal network is exponential. Thus, the currently equal discretization method does not improve the thermal estimation accuracy and reduce computational burdens simultaneously, where a trade-off must be taken between them. And due to the above assumption in the conventional methods, the currently equal discretization method not only degrades the estimation accuracy of the maximum and the minimum junction temperatures (T_{jmax}, T_{jmin}), but also changes the power-on time t_{on} of thermal behaviors as shown in Fig. 1. According to [21], [23], all of the T_{jmax}, T_{jmin}, and t_{on} are of significance for reliability evaluation. Therefore, achieving high-fidelity estimation of all these three thermal parameters (i.e., T_{jmax}, T_{jmin}, and t_{on}) with

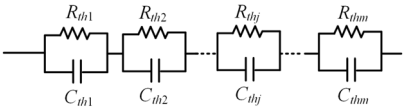

Fig.2. Foster-type thermal network.

less computational burdens is critical and has not been fully investigated.

To fulfill the aforementioned theoretical gap, this paper proposes a novel three-pulse equivalent power loss profile. By contrast to the conventional studies to equally divide the power losses, the proposed method of this paper discretizes the power loss by identifying the exact occurrences of the maximum and the minimum junction temperatures (i.e., t_{max}, t_{min}). This new discretization method decouples the conventional conflict between the thermal estimation accuracy and computational burdens and provides three advantages compared to the prior arts: 1) improve the accuracy of the thermal estimation, especially for the maximum and the minimum junction temperatures (i.e., T_{jmax}, T_{jmin}), 2) keep the high-fidelity of the power-on time (t_{on}) of thermal behaviors, and 3) reduce the computational burdens.

The rest of this paper proceeds as follows: a mathematical modeling method is provided to analyze thermal characteristics (t_{max}, t_{min}) and their main influences in Section II. Based on the obtained thermal characteristics, Section III presents a novel three-pulse equivalent power loss profile, in which two typical thermal characteristic scenarios are considered to make this method applicable to different time scales. Moreover, the equivalent values of each rectangular pulse losses are solved according to the principle of the same energy. In section IV, thermal matrix of IGBT (insulated gate bipolar transistor) model with a heat sink is extracted through the finite-element method. Then simulations and experimental tests are performed to verify the effectiveness of the proposed method. Further, the impact of thermal estimation with different methods on the lifetime evaluation is analyzed in Section V. Section VI provides the concluding remarks.

II. Thermal Characteristics Analysis

Different from the previous studies of dividing the power losses equally, this section aims to develop a method to identify the exact occurrences of the maximum and the minimum junction temperatures. First, the details of junction temperature dynamics during a period of the fundamental frequency are quantified by the generic discretization-integration process. Second, the exact occurrences of the maximum and the minimum junction temperatures are identified. The relevant variables which affect thermal characteristics are investigated. In addition, an indispensable variable ΔT_{j_in} (i.e., the difference between the initial junction temperature of steady-state thermal cycle and the reference temperature) is analyzed based on the proposed iterative model.

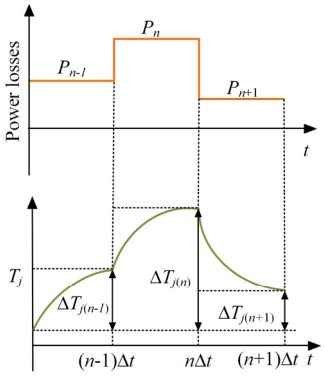

Fig. 3. Conversion from power losses to thermal profiles.

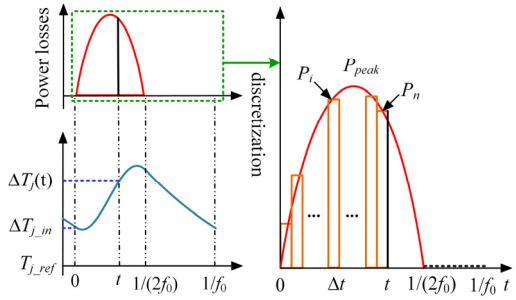

Fig. 4. Discretization of the half-sine loss profile.

A. Thermal Networks and Modeling Theory

Two commonly-used thermal networks are Cauer and Foster models [24]. However, Cauer model requires detailed information (e.g., geometrical size and materials) of each physical layer of power devices, which are usually difficult to access and limit its application scope in practice. On the contrast, Foster RC network is easy to be extracted from measured transient thermal responses and widely used for fast temperature estimation as shown in Fig. 2. Thus, the Foster RC network is employed in the following analysis with the following expression.

$$Z_{th}(t)=\sum_{j=1}^{m}R_{thj}(1-e^{-\frac{t}{\tau_{thj}}}) \tag{1}$$

where R_{thj}, τ_{thj} are the thermal resistance and thermal time constant of j-th RC lump, respectively. m is the order of Foster RC lumps.

Next, the junction temperature of power devices is estimated as shown in Fig. 3. The power losses are a series of rectangular pulses. By the references [25], [26], the corresponding thermal responses are expressed as

$$\begin{cases}\Delta T_{j(n-1)}=P_{n-1}R_{th}(1-e^{-\frac{\Delta t}{\tau_{th}}})\\ \Delta T_{j(n)}=\Delta T_{j(n-1)}e^{-\frac{\Delta t}{\tau_{th}}}+P_nR_{th}(1-e^{-\frac{\Delta t}{\tau_{th}}})\end{cases} \tag{2}$$

where $\Delta T_{j(n-1)}$ and P_{n-1} are the previous temperature fluctuation and the power loss, respectively. $\Delta T_{j(n)}$ is the present temperature fluctuation and P_n is the present power loss.

B. Locating the Occurrences of t_{max} and t_{min}

Selecting a single fundamental period and a random time point (the solid black line), as illustrated in Fig. 4, the power loss curve within the selected period is discretized into n rectangular pulse losses. Combined with (2), the junction temperature fluctuation at any time point $\Delta T_j(t)$ (the difference between the junction temperature and the reference temperature) can be solved, as shown in (3).

$$\Delta T_j(t)=\sum_{j=1}^{m}\left[\sum_{i=0}^{n-1}\left\{P_{i+1}R_{thj}e^{-\frac{(n-i)\Delta t}{\tau_{thj}}}(e^{\frac{\Delta t}{\tau_{thj}}}-1)\right\}+\Delta T_{j\_in}e^{-\frac{n\Delta t}{\tau_{thj}}}\right] \tag{3}$$

$$P_{i+1}=P_{peak}\sin[(2i+1)\pi f_0\Delta t] \tag{4}$$

where P_{peak} is the peak value of half-sine power loss, $P_{peak}=\pi\cdot P_{ave}$, P_{ave} is the average loss value within a fundamental period. The detailed derivation can be found in [19]. ΔT_{j_in} is the difference between the initial junction temperature of the steady-state thermal cycle and the reference temperature. The detailed calculation process of ΔT_{j_in} is illustrated in Part C of Section II.

In general, the greater number of discrete rectangular pulse losses, the better coincidence between the equivalent and original power loss profile. Thus, the junction temperature in (3) can be re-expressed as (5) when the number of discretized power losses approaches infinity.

$$\Delta T_j(t)=\sum_{j=1}^{m}\left\{\begin{aligned}&e^{-\frac{t}{\tau_{thj}}}\int_0^t\left[\frac{R_{thj}P_{peak}}{\tau_{thj}}e^{\frac{u}{\tau_{thj}}}\sin(2\pi f_0u)\right]du\\&+\Delta T_{j\_in}e^{-\frac{t}{\tau_{thj}}}\end{aligned}\right\} \tag{5}$$

By solving the first-order derivative of (5) expressed as (6), the time point of unique maximum and minimum junction temperature can be located accurately. It can be seen that thermal characteristics are affected by some factors, such as thermal resistance R_{thj}, thermal time constant τ_{thj}, the peak value of the half-sine power loss P_{peak}, the fundamental frequency f_0, and the initial temperature difference ΔT_{j_in}.

C. ΔT_{j_in} Modeling Analysis

For the aforementioned factors, ΔT_{j_in} is not directly available. To simply obtain ΔT_{j_in}, this part proposes a simplified iterative calculation method. As shown in Fig. 5,

$$\Delta T_j'(t)=\sum_{j=1}^{m}\left\{\frac{R_{thj}P_{peak}}{\tau_{thj}}\sin(2\pi f_0t)-\frac{R_{thj}P_{peak}}{\tau_{thj}\left[1+(2\pi f_0\tau_{thj})^2\right]}\left\{\sin(2\pi f_0t)-2\pi f_0\tau_{thj}\left[\cos(2\pi f_0t)-e^{-\frac{t}{\tau_{thj}}}\right]\right\}-\frac{\Delta T_{j\_in}}{\tau_{thj}}e^{-\frac{t}{\tau_{thj}}}\right\} \tag{6}$$

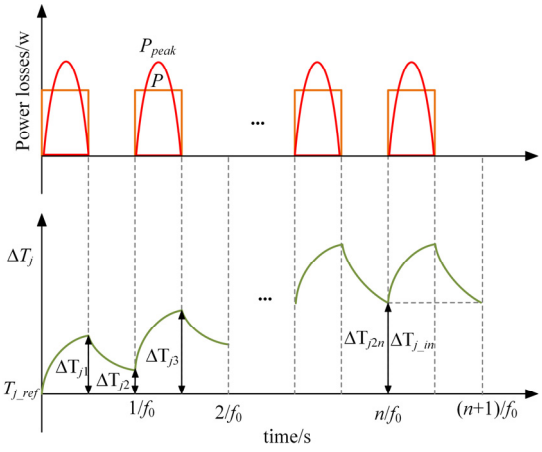

Fig. 5. Schematic diagram of the junction temperature transition from the transient stage to the steady-state stage under the square-wave losses.

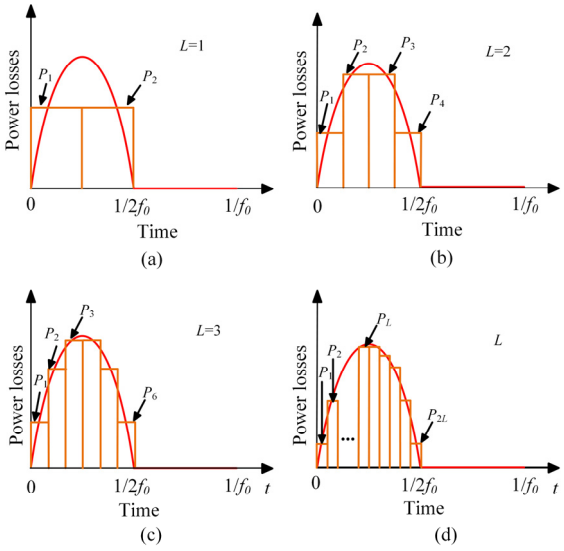

Fig. 6. Existing thermal modeling, where L is the number of the divided dissipation levels, P_1, P_2,..., P_L,..., P_{2L} are the divided dissipation pules: (a) one level loss (i.e., square-wave loss), (b) two-level losses, (c) three-level losses, (d) L-level losses.

the half-sine power loss is converted to the square wave power loss. Since the two loss models share the same energy, heating time, and cooling time in one fundamental period, the obtained junction temperature through the two models is almost consistent at the end of the fundamental period.

Fig. 5 presents the square-wave power loss with the amplitude of P and the calculated IGBT junction temperature with the junction temperature being the reference temperature. It is assumed that the junction temperature of the module reaches a steady-state at the nth fundamental period.

Taking $1/(2f_0)$ as the iterative period, the junction temperature after each iteration can be expressed as

$$\begin{cases} \Delta T_{j1} = \sum_{j=1}^{m}\left[PR_{thj}(1-e^{-\frac{1}{2\tau_{thj}f_0}}) \right] \\ \Delta T_{j2} = \sum_{j=1}^{m}\left[PR_{thj}(1-e^{-\frac{1}{2\tau_{thj}f_0}})e^{-\frac{1}{2\tau_{thj}f_0}} \right] \\ \Delta T_{j3} = \sum_{j=1}^{m}\left[PR_{thj}(1-e^{-\frac{1}{2\tau_{thj}f_0}}) + \Delta T_2 e^{-\frac{1}{2\tau_{thj}f_0}} \right] \\ \vdots \\ \Delta T_{j2n} = \sum_{j=1}^{m}\left[PR_{thj}(1-e^{-\frac{1}{2\tau_{thj}f_0}})e^{-\frac{1}{2\tau_{thj}f_0}} + \sum_{i=0}^{n} e^{-\frac{1}{2\tau_{thj}f_0}} \right] \end{cases} \tag{7}$$

Given the same energy of the two power loss models, the relationship between the square wave loss value P and the peak value of half-sine power loss P_{peak} can be solved.

$$P = \frac{2P_{peak}}{\pi} \tag{8}$$

When n approaches infinity, the final steady-state ΔT_{j_in} can be extracted as

$$\Delta T_{j\_in} = \sum_{j=1}^{m}\left[\frac{2R_{thj}P_{peak}(e^{-\frac{1}{2\tau_{thj}f_0}} - e^{-\frac{2}{2\tau_{thj}f_0}})}{\pi(1-e^{-\frac{1}{\tau_{thj}f_0}})} \right] \tag{9}$$

Substituting (9) into (6), the conclusion can be drawn that the occurrences of the two key thermal stresses are irrelevant to the power loss amplitude and only depend on thermal network parameters and fundamental frequency.

At the same time, considering the practical application of the proposed method, the changes of these influences are fully considered. For fundamental frequency, it can be captured through control strategies, such as PLL (phase-locked loop) [27]. As for thermal parameters, they are mainly influenced by aging, which can be considered through updating thermal network parameters. The updated methods have been provided in [28], [29]. And the analysis of this paper has chosen the easily extracted Foster RC network.

III. Three-Pulse Equivalent Power Loss Profile

Based on the thermal characteristics obtained in the previous section, a new opportunity is provided for simplified thermal modeling. Different from the existing discretization methods, which equally divides power loss profiles as shown in Fig. 6. It can be seen that the duration of each divided dissipation pules is equal. This paper determines the intervals of each equivalent step of power loss based on the identified occurrences of maximum and minimum thermal stresses.

Taking a fundamental period as an example, the proposed simplified thermal modeling is shown in Fig. 7. In order to make the proposed method better generality, thermal characteristics under different time scales (i.e., different fundamental periods) are considered, which include two typical scenarios. The first scenario has the unique maximum and minimum thermal stresses, as shown in Fig. 7 (a). And the power loss profile can be discretized into three rectangular

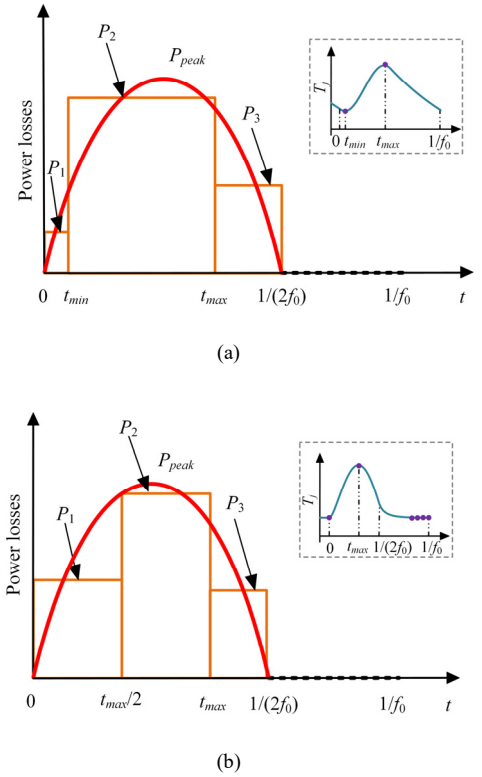

Fig. 7. Proposed simplified thermal modeling based on thermal characteristics; (a) t_{max}, t_{min} are considered, (b) t_{max} is considered.

pules. Meanwhile, Fig. 7 (b) shows another scenario, there are multiple minimum thermal stresses, one of them appears at the beginning of the fundamental period, and the rest appears after 1/2 fundamental period. But the maximum thermal stress is unique. Because there is only one reference point from 0 to 1/2 of the fundamental period. The numbers of discretization in this scenario should be set to two. However, the greater number of divisions results in a more accurate junction temperature estimation [22]. In order to improve the estimation accuracy while maintaining the same computational efforts with Fig. 7 (a), $t_{max}/2$ (i.e., the time point of the half-time interval of t_{max}) is introduced as another reference time point.

Assuming that $u = t_{min} / t_0$ and $w = t_{max} / t_0$ respectively. According to the principle of the same energy, the values of divided dissipation pulses can be solved by the following functions.

Considering t_{min} and t_{max} (scenario (a)), it can be obtained as

$$\begin{cases} \dfrac{P_1 u}{f_0} = \int_0^{u/f_0} P_{peak}\sin(2\pi f_0 t)dt \\ \dfrac{P_2(w-u)}{f_0} = \int_{u/f_0}^{w/f_0} P_{peak}\sin(2\pi f_0 t)dt \\ \dfrac{P_2(0.5-w)}{100 f_0} = \int_{w/f_0}^{1/(2f_0)} P_{peak}\sin(2\pi f_0 t)dt \end{cases} \tag{10}$$

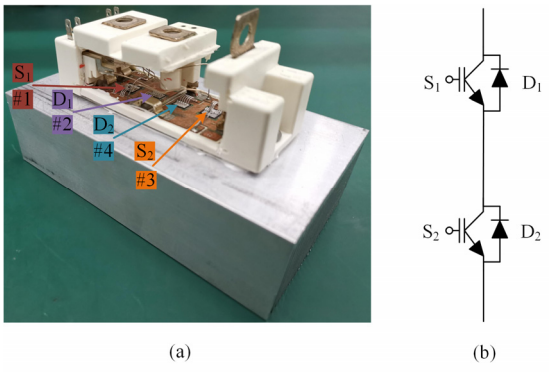

Fig. 8. Analyzed power semiconductor module with heatsink. (a) lateral structure; (b) circuit topology diagram of power module.

Considering t_{max} /2 and t_{max} (scenario (b)), it can be given.

$$\begin{cases} \dfrac{P_1 w}{2 f_0} = \int_0^{w/(2f_0)} P_{peak}\sin(2\pi f_0 t)dt \\ \dfrac{P_2 w}{2 f_0} = \int_{w/(2f_0)}^{w/f_0} P_{peak}\sin(2\pi f_0 t)dt \\ \dfrac{P_2(0.5-w)}{100 f_0} = \int_{w/f_0}^{1/(2f_0)} P_{peak}\sin(2\pi f_0 t)dt \end{cases} \tag{11}$$

Furthermore, the values of each rectangular loss pulses in two scenarios are obtained.

Scenario (a):

$$\begin{cases} P_1 = \dfrac{1-\cos(2\pi u)}{2\pi u} P_{peak} \\ P_2 = \dfrac{\cos(2\pi u)-\cos(2\pi w)}{2\pi(w-u)} P_{peak} \\ P_3 = \dfrac{1+\cos(2\pi w)}{2\pi(0.5-w)} P_{peak} \end{cases} \tag{12}$$

Scenario (b):

$$\begin{cases} P_1 = \dfrac{1-\cos(\pi w)}{\pi w} P_{peak} \\ P_2 = \dfrac{\cos(\pi w)-\cos(2\pi w)}{\pi w} P_{peak} \\ P_2 = \dfrac{1+\cos(2\pi w)}{2\pi(0.5-w)} P_{peak} \end{cases} \tag{13}$$

IV. Simulation and Experimental Results

Simulation and experiments considering different frequency scales are implemented to validate the proposed method. And the estimated junction temperatures are compared with the existing two commonly accepted discretization models. In addition, for indispensable elements in junction temperature calculation, the parameters of thermal matrix, which take account of the heat sink, are extracted through the finite element method, COMSOL.

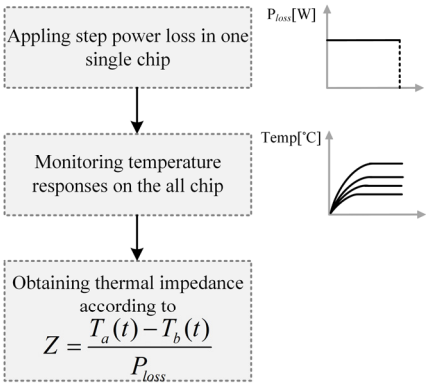

Fig. 9. Flowchart of the thermal impedance obtaining approach.

A. Thermal Matrix

Before validating the proposed thermal modeling method, thermal matrix is established. Thermal matrix based on superposition law [30] can achieve accurate junction temperature calculation due to considering the thermal coupling effect among devices. An IGBT module from Infineon, rated at 50 A and 1200 V (FF50R12RT4), is taken as a case study [31]. The IGBT module contains two IGBT chips and two anti-parallel diode chips. Fig. 8 shows the lateral structure and circuit topology of the IGBT model with the heat sink. To facilitating the experimental implementation and calculation of junction temperature, the thermal impedance from junction to ambient (Z_{th_ja}), is extracted based on the finite-element method (FEM), namely, COMSOL. Therefore, in the multi-physical field analysis, the ambient temperature is selected as the reference temperature (T_{j_ref}). The junction temperature heating curves have been used to obtain the thermal impedance [32]. Fig. 9 presents the flowchart of the thermal impedance obtaining approach. A step response analysis is performed for all chips, by applying the step power loss input to one single chip and then monitoring the temperature responses on the all chips. Due to geometrical symmetries of the module and heat sink, only one IGBT (S_1) and anti-parallel diode (D_1) are selected to apply heating loss. The results are a series of curves, which are transient temperature responses. Next, the transient thermal impedance curves are extracted by [24]

$$Z = \frac{T_a(t) - T_b(t)}{P_{loss}} \tag{14}$$

where $T_a(t)$ and $T_b(t)$ are the temperatures of corresponding chips and reference point respectively and P_{loss} is the applied step power loss.

According to the obtained thermal impedances and geometrical symmetries, the junction temperature on each chip is expressed as (15) [33], [34].

B. Simulation Analysis

To verify the estimated performance of junction temperature, simulations are implemented. And Fig. 10 presents the flowchart of the estimated temperature obtaining

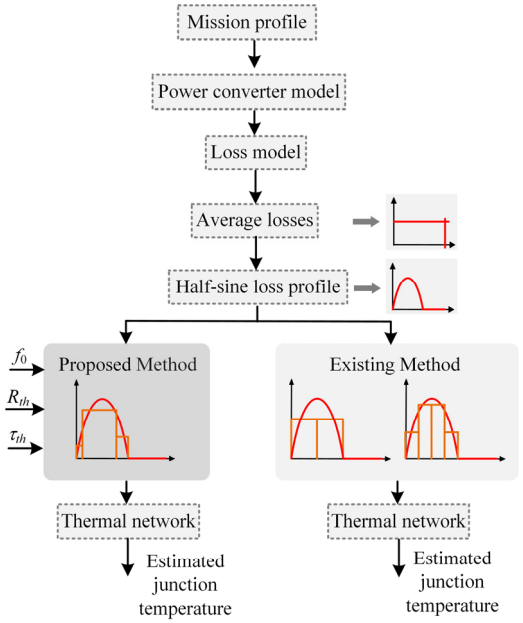

Fig.10. Flowchart of the estimated temperature based on different equivalent principles.

$$\begin{bmatrix} T_{j1} \\ T_{j2} \\ T_{j3} \\ T_{j4} \end{bmatrix} = \begin{bmatrix} Z_{th11} & Z_{th12} & Z_{th13} & Z_{th14} \\ Z_{th21} & Z_{th22} & Z_{th23} & Z_{th24} \\ Z_{th13} & Z_{th14} & Z_{th11} & Z_{th12} \\ Z_{th23} & Z_{th24} & Z_{th21} & Z_{th22} \end{bmatrix} \begin{bmatrix} P_1 \\ P_2 \\ P_3 \\ P_4 \end{bmatrix} + T_{j\_ref} \tag{15}$$

approach based on different equivalent principles. In order to find a half-sine power loss profile, the IGBT module is loaded with a three-phase two-level grid-side inverter [35]. The detailed inverter specifications are listed in Table I. Combining with operating parameters, the average losses value within a fundamental period is calculated [20], which is 50 W. Then the half-sine loss is discretized based on different equivalent principles, and the obtained step power losses are used as the input of thermal network to obtain the corresponding estimated junction temperature.

TABLE I
PARAMETERS OF INVERTER

DC bus voltage	600 V
Rated primary side voltage	380 V
Load current	40 A
Output power factor	1.0
Switching frequency	2.0 kHz
Filter inductance	1.9 mH
IGBT module	1200 V/50 A

Before conducting a comparative analysis of estimated junction temperature, the evaluation criterion is provided and defined as (16) [22]. The relative estimation error of the junction temperature fluctuation is used as the evaluation criterion, which involves maximum and minimum junction

temperature. And the junction temperature with the half-sine loss model is regarded as the reference.

$$\varepsilon = \frac{(T_{j\max\text{-}hs} - T_{j\max}) - (T_{j\min\text{-}hs} - T_{j\min})}{T_{j\max\text{-}hs} - T_{j\min\text{-}hs}} \tag{16}$$

where $T_{jmax\text{-}hs}$ and $T_{jmin\text{-}hs}$ represent the maximum and minimum junction temperatures under half-sine power loss profile, respectively. T_{jmax} and T_{jmin} represent the maximum and minimum junction temperatures calculated by different equivalent thermal models.

Fig. 11 shows the steady-state thermal behaviors at four typical fundamental frequencies. The existing model [22] with the divided dissipation level, k=1 and 2, is implemented as a performance comparison with the proposed model. And as for the computational burden, it is closely related to the number of divided dissipation pules. More specifically, there are two and four computational cycles under the existing models respectively, while the proposed model has three computational cycles in a single fundamental period.

According to the comparsion of the error ε in Fig. 11, it can be seen that the proposed model can achieve smaller estimation errors. For example, the errors of 7.96% under the existing models with k=2 are improved and reach 6.13% with the proposed model at 1 Hz, 8.32%, and 0.74% present a sharp contrast at 50 Hz. And the proposed model has the less computational burden. When comparing with the existing model with k=1, the proposed model has a more obvious accuracy advantage (33.90% and 6.13%, 9.83%, and 0.74%). According to the above comparison of the thermal estimation accuracy and computational burdens, it can be concluded that the proposed model decouples the conventional conflict of two parts in the existing models. In other words, the proposed method achieves the improvement of thermal estimation accuracy and the reduction of computational burdens simultaneously. Moreover, it is more convenient in practice to use a general simplified model instead of dynamically adjusting the simplified models (multiple models) to meet the allowable error, especially under varied-frequency applications. For example, the existing method requires k=2 at 1 Hz and 5 Hz, and k=1 at 50 Hz and 100 Hz respectively if the accepted error is 10%. In addition, for typical fundamental frequencies (50 Hz), the existing methods should pay more computational efforts if the error reaches the same level as the proposed method.

In order to verify the proposed method under extensive fundamental frequency scales, Fig. 12 analyzes the estimation error under twelve fundamental frequencies. No significant error improvement is found only when f_0 = 10 Hz. Simultaneously, Fig. 13 shows the transient state thermal performances under two fundamental frequencies, it can be seen the comparison of ε that the proposed method can also achieve better thermal estimation performance than the existing methods. In all, it confirms that the proposed method can offer a more accurate estimation of the junction temperature fluctuation with less computational effort. At the same time, thermal characteristics are presented under extensive fundamental frequencies, as shown in Fig. 14. It can

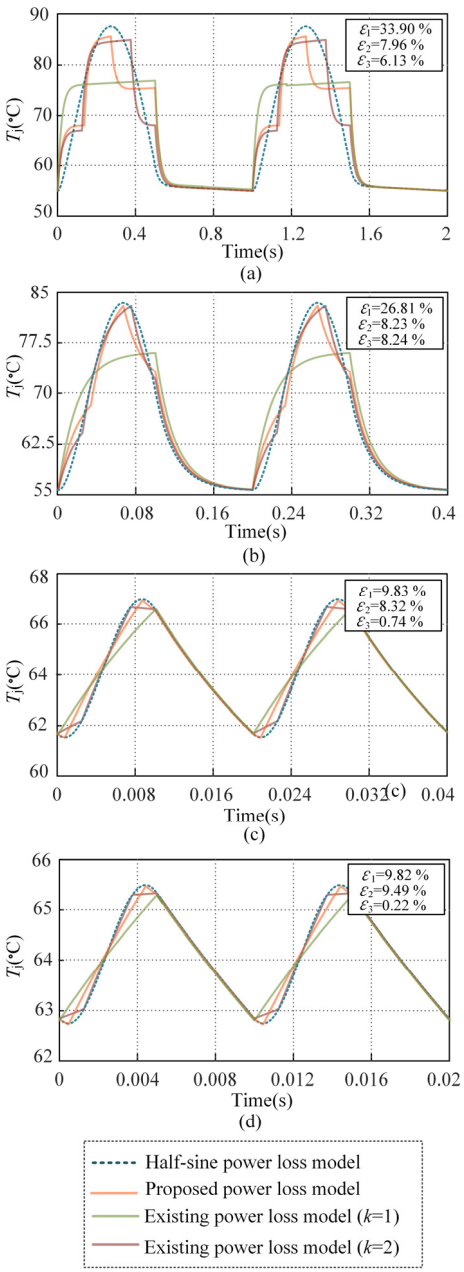

Fig.11. Steady-state simulation results under four fundamental frequencies, where ε_1 and ε_2 are the corresponding errors when the divided dissipation level k = 1 and 2 under the existing model, respectively, ε_3 is the error while applying the proposed model; (a) 1 Hz, (b) 5 Hz, (c) 50 Hz, (d) 100 Hz.

be seen that both u and w will increase with the fundamental frequency. And the distinctive performance (i.e., only t_{max}, t_{min}, and only t_{max}) has also been verified by the thermal characteristic classification in Section III.

As for power-on time, formula (17) is used to analyze its error.

$$\delta = \frac{t_{on-hs} - t_{on}}{t_{on-hs}} \tag{17}$$

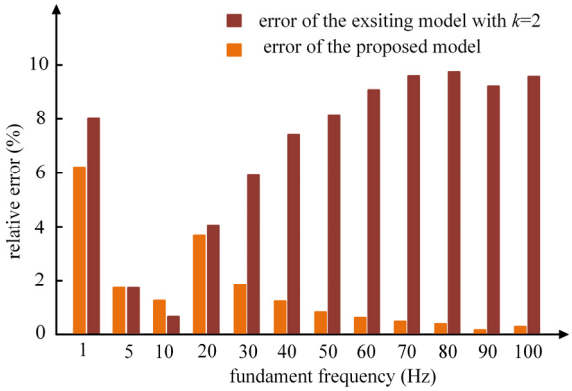

Fig.12. Error analysis under extensive fundamental frequencies with two discretization models, which are the proposed model and the existing model with k=2 [22], respectively.

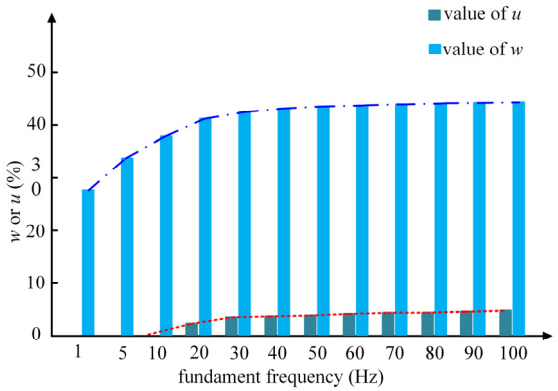

Fig.14. Thermal characteristics under extensive fundamental frequencies; where $u = t_{min} / t_0$ and $w = t_{max}/t_0$, t_{max} and t_{min} are the occurrences of maximum and minimum junction temperature respectively, t_0 is fundamental period.

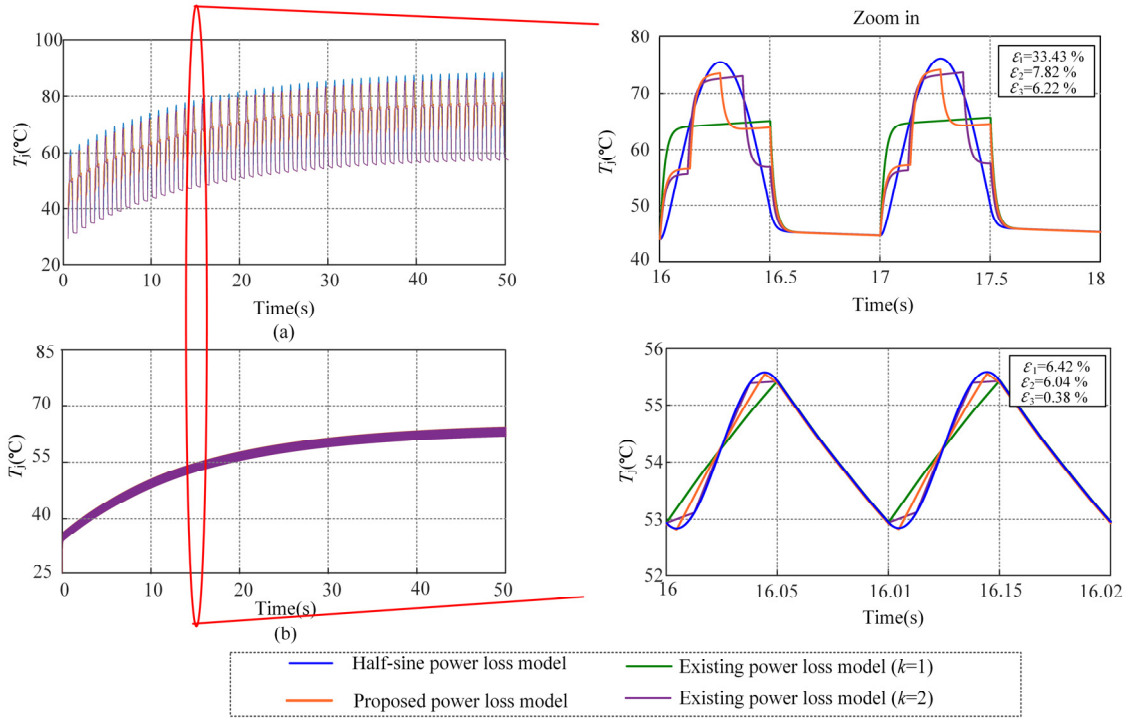

Fig. 13 Transient state simulation results under two fundamental frequencies, where ε_1 and ε_2 are the corresponding errors when the divided dissipation level k = 1 and 2 under the existing model, respectively, ε_3 is the error while applying the proposed model; (a) 1 Hz, (b) 100 Hz.

where $t_{on\text{-}hs}$ represents the power-on time under the half-sine power loss profile. t_{on} is the power on time under different equivalent thermal models.

Table II presents the error of t_{on} under the existing model in steady-state. It is noteworthy that the proposed thermal model can keep the high-fidelity of $t_{on\text{-}hs}$ through the proposed location method in section II. $\delta 1$ and $\delta 2$ represent the error of power on time under the existing model with k=1, k=2, respectively. The obvious errors indicate that the existing model has poor performance on t_{on}.

TABLE II
ERROR OF POWER ON TIME UNDER EXISTING MODEL

Fundamental frequency (Hz)	$\delta 1$ (%)	$\delta 2$ (%)
1	-83.04	-37.28
5	-49.36	-12.02
50	-29.03	3.23
100	-25.89	5.58

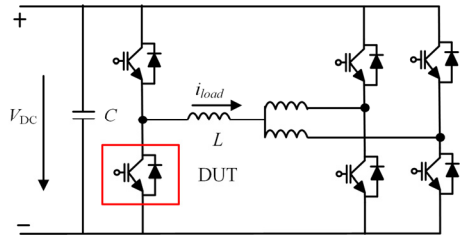

Fig.15. Schematic of inverter.

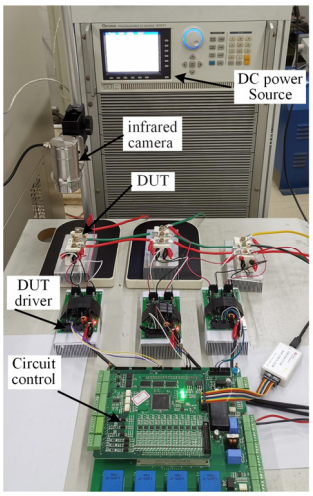

Fig.16. Experimental platform for the thermal behavior evaluation.

The proposed model, achieving high-fidelity estimation of all these concerned thermal parameters (i.e., T_{jmax}, T_{jmin}, and t_{on}) with less computational burdens, mainly benefits from the exact determination of the occurrences of the maximum and minimum junction temperature and more reasonable discretization for power losses based on them. And according to the above analysis, this novel three-pulse discretization method completely solves the conventional conflict between the computational burdens and thermal estimation accuracy.

C. Experimental Validations

To demonstrate the effectiveness of the proposed method, experimental tests are implemented. The IGBT in the three-phase inverter is selected as a case study and the schematic of the inverter is shown in Fig. 15. Moreover, the parameters of the experiment setup are listed in Table III. Fig. 16 presents the experimental platform for the thermal-behavior evaluation.

TABLE III
PARAMETERS OF THE INVERTER

Parameter	Value
DC bus voltage V_{DC}	240 V
Load current i_{load}	16 A (RMS)
Fundamental frequency f_0	1 Hz, 5Hz
Inductor L	3 mH
Switching frequency f_s	2.5 kHz
IGBT module	50 A/1200 V

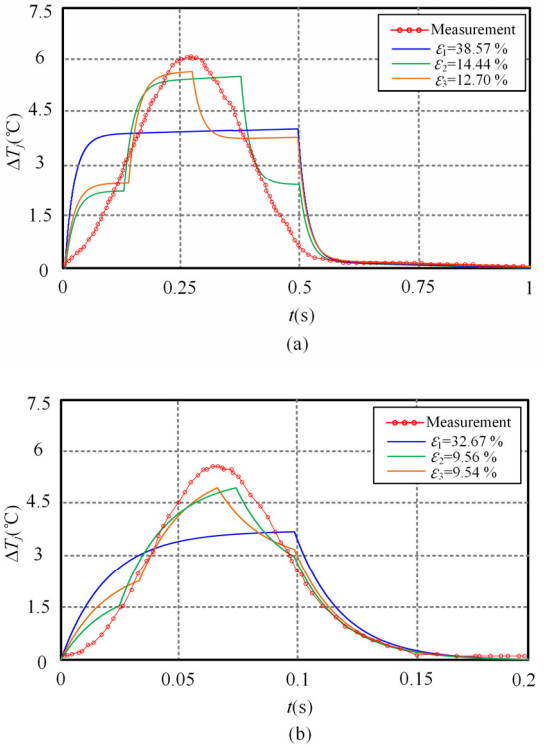

Fig. 17. Measured junction temperature profiles and the estimated thermal profile with different thermal models at two fundamental frequencies, where ε_1 and ε_2 are the corresponding errors when the divided dissipation level k = 1 and 2 under the existing model, respectively, ε_3 is the error while applying the proposed model; (a) 1Hz, (b) 5 Hz.

An opened IGBT module is tested in the experimental platform. The lower chip in the IGBT module is regarded as the device under test (DUT), where the junction temperature is measured by an infrared camera. The inverter operates at 1 Hz and 5 Hz due to the limitation of the sampling frequency of the infrared camera.

It can be seen from Fig. 17 that the proposed model can achieve better estimation performance than that of the existing model. And, it has a minimal error (12.7%) and improves significantly the error of 38.57% under the existing model, which is achieved only by adding one computational cycle. At the same time, compared with k=2, it also improves the accuracy of estimation while reducing the computational burden. And the fundamental frequency of 5 Hz also has the same performance. Moreover, the proposed thermal model keeps the power-on time (t_{on}) consistent with actual thermal behaviors. From experimental results, it is further confirmed that the proposed method can offer a more accurate estimation of the junction temperature fluctuation.

V. IMPACT OF THERMAL ESTIMATION ON THE LIFETIME EVALUATION

In practice, applying the estimated junction temperature to reliability analysis is more concerned. Therefore, this section

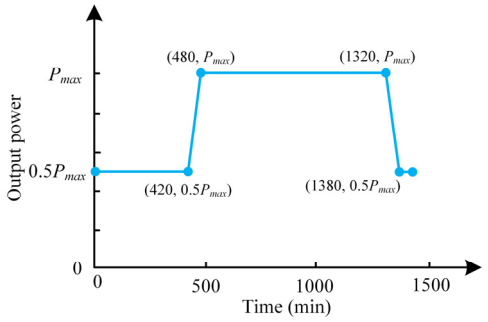

Fig.18. One-day grid-side inverter output power profile.

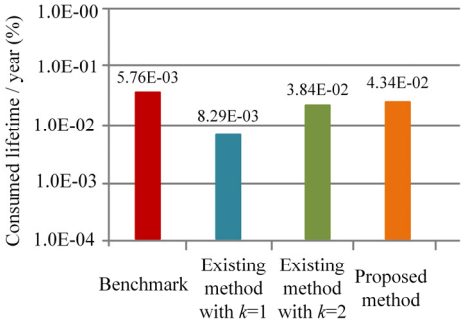

Fig.19. Consumed lifetime of IGBT based on different methods.

presents the impact of junction temperature estimation errors with the different methods on lifetime evaluation.

The IGBT module in the case study of simulation analysis is selected as the subject investigated. In this paper, the damage evaluation of the power modules is based on this mission profile, a simple one-day output power profile, as depicted in Fig. 18 [36]. P_{max} is the maximum output power of the grid-side inverter, which matches the parameters given in Table I. And the fundamental frequency is 1 Hz. The commonly-employed lifetime model, Bayerer's Model, which considers the impact of minimum junction temperature, junction temperature fluctuations and the power-on time, is used to analyze [37]. Fig. 19 shows the consumed lifetime (i.e., annual damage) based on three methods, where the obtained result of half-sine loss profile is regarded as the benchmark, and Table IV provides the lifetime evaluation results.

TABLE IV
LIFETIME EVALUATION RESULTS WITH DIFFERENT METHODS

Methods	Lifetime (year)
Benchmark	17.34
Existing method with k=1	120.69
Existing method with k=2	26.03
Proposed method	23.03

According to the comparison, it can be seen that the evaluated result based on the proposed method is more accurate and closer to the benchmark. If applying the existing method with k=1, larger errors are observed than the benchmark. And the lifetime result far exceeds the practically expected IGBT module lifetimes, which easily causes the misjudgment of guidance to reliability engineers. Thus, the existing model with k=1 (i.e., square-wave loss profile) fails in junction temperature estimation and lifetime evaluation despite its computational advantages. Compared with the proposed method, the existing method with k=2 not only still has a certain error in lifetime evaluation, but also requires more computational efforts. Therefore, it can be concluded that the thermal estimation advantages of the proposed method further contribute to better performance in the lifetime evaluation.

VI. Conclusion

This paper has proposed a simplified thermal modeling method considering the thermal characteristics of power device (i.e., the occurrences of the maximum and the minimum junction temperature). First, to locate the two key time points of the maximum and minimum junction temperatures, a generic mathematical model has been investigated. For thermal modeling, instead of equally dividing power losses conventionally, the proposed method discretized the power loss profile into unequal three pulses based on the previously obtained thermal characteristics. The proposed equivalent power loss profile firstly decouples the conventional conflict between the thermal estimation accuracy and computational burdens. In other words, while the conventional methods improve accuracy at the cost of increasing the discrete power-loss pulses (i.e., increased computations), the proposed method can use a three-pulse equivalent power loss profile under varied conditions. As a result, both improving the accuracy of the thermal estimation and reducing computations can be achieved simultaneously. Moreover, the proposed method maintains the high fidelity of the power-on time of the thermal profile. To consider different time scales, two typical scenarios of thermal characteristics have been discussed as well. Finally, this paper compares the conventional methods with the proposed method through both simulations and a 26-kW three-phase experimental platform. The performances of the proposed method have been verified. For instance, when k=2 and f=50Hz, the proposed method contributes to reducing thermal estimation error from 8.32% conventionally to 0.75%, decreasing computations by 25%, and keeping power-on time consistent with reality, respectively. And these better thermal estimation performances are further reflected in the lifetime evaluation, and providing a more convincing result.

References

[1] H. Wang, M. Liserre, and F. Blaabjerg, "Toward reliable power electronics: challenges, design tools, and opportunities," *IEEE Ind. Electron. Mag.*, vol. 7, no. 2, pp. 17-26, Jun. 2013.

[2] S. Yang, A. Bryant, P. Mawby, D. Xiang, L. Ran, and P. Tavner, "An industry-based survey of reliability in power electronic converters,"

IEEE Trans. Ind. Appl., vol. 47, no. 3, pp. 1441–1451, May/Jun. 2011.
[3] E. Wolfgang, "Examples for failures in power electronics systems," presented at *ECPE tutorial on reliability of power electronic systems*, Nuremberg, Germany, 2007.
[4] H. Wang and F. Blaabjerg, "Power electronics reliability: state of the art and outlook," *IEEE J. of Emerg. and Sel. Topics in Power Electron.*, *early access*, doi: 10.1109/JESTPE.2020.3037161.
[5] C. V. Pop, A. Buzo, G. Pelz, H. Cucu and C. Burileanu, "The estimation of the lifetime variation for power devices," *IEEE Trans. Device Mater. Rel*., vol. 19, no. 4, pp. 654-663, Dec. 2019.
[6] M. Liserre, G. Buticchi, J. I. Leon, A. M. Alcaide, V. Raveendran, Y. K, et al., "Power routing: A new paradigm for maintenance scheduling," *IEEE Ind. Electron. Mag.*, vol. 14, no. 3, pp. 33-45, Sep. 2020.
[7] B. Yao, X. Ge, X. Dong, S. Li, Y. Zhang, H. Wang and H. Wang, "Electro-thermal stress analysis and lifetime evaluation of DC-link capacitor banks in the railway traction drive system," *IEEE J. of Emerg. and Sel. Topics in Power Electron.*, *early access*, doi: 10.1109/JESTPE.2020.3000130.
[8] A. Hanif, Y. Yu, D. DeVoto, and F. Khan, "A comprehensive review toward the state-of-the-art in failure and lifetime predictions of power electronic devices," *IEEE Trans. Power Electron*, vol. 34, no. 5, pp. 4729-4746, May. 2019.
[9] S. Peyghami, H. Wang, P. Davari, and F. Blaabjerg, "Mission-profile-based system-level reliability analysis in DC micro-grids," *IEEE Trans. Ind. Appl.*, vol. 55, no. 5, pp. 5055-5067, Sep./Oct. 2019.
[10] A. Sangwongwanich, Y. Yang, D. Sera, and F. Blaabjerg, "Lifetime evaluation of grid-connected PV inverters considering panel degradation rates and installation sites," *IEEE Trans. Power Electron*, vol. 33, no. 2, pp. 1225-1236, Feb. 2018.
[11] Y. Zhang, H. Wang, Z. Wang, F. Blaabjerg and M. Saeedifard, "Mission profile-based system-level reliability prediction method for modular multilevel converters," *IEEE Trans. Power Electron*, vol. 35, no. 7, pp. 6916-6930, Jul. 2020.
[12] Y. Zhang, H. Wang, Z. Wang, Y. Yang and F. Blaabjerg, "Simplified thermal modeling for IGBT modules with periodic power loss profiles in modular multilevel converters," *IEEE Trans. Ind. Electron.*, vol. 66, no. 3, pp. 2323-2332, Mar. 2019.
[13] K. Ma, M. Liserre, F. Blaabjerg, and T. Kerekes, "Thermal loading and lifetime estimation for power device considering mission profiles in wind power converter," *IEEE Trans. Power Electron*, vol. 30, no. 2, pp. 590-602, Feb. 2015.
[14] P. D. Reigosa, H. Wang, Y. Yang and F. Blaabjerg, "Prediction of bond wire fatigue of IGBTs in a PV inverter under a long-term operation," *IEEE Trans. Power Electron*, vol. 31, no. 10, pp. 7171-7182, Dec. 2016.
[15] W. Lai, M. Chen, L. Ran, O. Alatise, S. Xu and P. Mawby, "Low ΔT_j stress cycle effect in IGBT power module die-attach lifetime modeling," *IEEE Trans. Power Electron*, vol. 31, no. 9, pp. 6575-6585, Sep. 2016.
[16] Y. Zhang, H. Wang, Z. Wang and F. Blaabjerg, "Computational-efficient thermal estimation for IGBT modules under periodic power loss profiles in modular multilevel converters," *IEEE Trans. Ind. Appl*., vol. 55, no. 5, pp. 4984-4992, Sep. /Oct. 2019.
[17] M. Musallam and C. M. Johnson, "Real-Time compact thermal models for health management of power electronics," *IEEE Trans. Power Electron*, vol. 25, no. 6, pp. 1416-1425, Jun. 2010.
[18] G. C. James, "Frequency domain temperature model—A new method in on-line temperature estimation for power modules in drives applications," Ph.D. dissertation, School Elect., Electron. Comput. Eng., *Newcastle Univ*., Newcastle upon Tyne, U.K., 2010.
[19] Infineon Application Note AN2008-03: Thermal equivalent circuit models, June 2008.
[20] A. Wintrich, N. Ulrich, T. Werner, and T. Reimann, *Application Manual Power Semiconductors*. Nuremberg, Germany: Semikron, 2015.
[21] K. Ma, A. S. Bahman, S. Beczkowski, and F. Blaabjerg, "Complete loss and thermal model of power semiconductors including device rating information," *IEEE Trans. Power Electron*, vol. 30, no. 5, pp. 2556-2569, May. 2015.
[22] Y. Zhang, H. Wang, Z. Wang, Y. Yang, and F. Blaabjerg, "A simplification method for power device thermal modeling with quantitative error analysis," *IEEE J. of Emerg. and Sel. Topics in Power Electron.*, vol. 7, no. 3, pp. 1649-1658, Sep. 2019.
[23] U. Choi, F. Blaabjerg, and K. Lee, "Study and handling methods of power IGBT module failures in power electronic converter systems," *IEEE Trans. Power Electron*, vol. 30, no. 5, pp. 2517-2533, May. 2015.
[24] Zhaohui Luo, Hyungkeun Ahn. and M. A. E. Nokali, "A thermal model for insulated gate bipolar transistor module," *IEEE Trans. Power Electron*, vol. 19, no. 4, pp. 902-907, Jul. 2004.
[25] N. Sintamarean, F. Blaabjerg, H. Wang, F. Iannuzzo, and P. P. Rimmen, "Reliability oriented design tool for the new generation of grid connected PV-inverters," *IEEE Trans. Power Electron*, vol. 30, no. 5, pp. 2635-2644, May. 2015.
[26] B. Yao, X. Ge, H. Wang, H. Wang, D. Zhou and B. Gou, "Multitimescale reliability evaluation of DC-Link capacitor banks in metro traction drive system," *IEEE Trans Transp. Electrific*., vol. 6, no. 1, pp. 213-227, Mar 2020.
[27] H. Wang, X. Ge, Y. Yue and Y. Liu, "Dual phase-locked loop-based speed estimation scheme for sensorless vector control of linear induction motor drives, *IEEE Trans. Ind. Electron.*, vol. 67, no. 7, pp. 5900-5912, July 2020, doi: 10.1109/TIE.2019.2952818.
[28] H. Chen, B. Ji, V. Pickert and W. Cao, "Real-time temperature estimation for power MOSFETs considering thermal aging effects," *IEEE Trans. Device Mater. Reliab*., vol. 14, no. 1, pp. 220-228, Mar. 2014.
[29] Z. Hu, M. Du, K. Wei and W. G. Hurley, "An adaptive thermal equivalent circuit model for estimating the junction temperature of IGBTs," *IEEE J. of Emerg. and Sel. Topics in Power Electron*., vol. 7, no. 1, pp. 392-403, Mar. 2019.
[30] Z. Khatir, S. Carubelli and F. Lecoq, "Real-time computation of thermal constraints in multichip power electronic devices," *IEEE Trans. Compon. and Packag. Technol*., vol. 27, no. 2, pp. 337-344, Jun. 2004.
[31] (2013). Infineon FF50R12RT4. [Online]. Available: https://www.infineon.com/dgdl/Infineon-FF50R12RT4-DS-v02_00en_cn.pdf.
[32] A. S. Bahman, K. Ma and F. Blaabjerg, "A lumped thermal model including thermal coupling and thermal boundary conditions for high-power IGBT modules," *IEEE Trans. Power Electron,* vol. 33, no. 3, pp. 2518-2530, Mar. 2018.
[33] A. S. Bahman, K. Ma, P. Ghimire, F. Iannuzzo and F. Blaabjerg, "A 3-D-lumped thermal network model for long-term load profiles analysis in high-power IGBT modules," *IEEE J. of Emerg. and Sel. Topics in Power Electron.*, vol. 4, no. 3, pp. 1050-1063, Sep. 2016.
[34] Y. Zhang, Z. Wang, H. Wang and F. Blaabjerg, "Artificial intelligence-aided thermal model considering cross-coupling effects," *IEEE Trans. Power Electron*, vol. 35, no. 10, pp. 9998-10002, Oct. 2020.
[35] B. Wen, D. Boroyevich, R. Burgos, P. Mattavelli and Z. Shen, "Analysis of D-Q small-signal impedance of grid-tied inverters," *IEEE Trans. Power Electron*, vol. 31, no. 1, pp. 675-687, Jan. 2016.
[36] Wang L, Xu J, Wang G, et al. "Lifetime estimation of IGBT modules for MMC-HVDC application", Microelectronics Reliability, 2018, 82:90-99.
[37] R. Bayerer, T. Hermann, T. Licht, J. Lutz, and M. Feller, "Model for power cycling lifetime of IGBT modules-Various factors influencing lifetime," in *Proc. Int. Conf. Integr. Power Syst.*, 2008, pp. 1–6.

Yichi Zhang (S'20) received the B.Eng. degrees in electrical engineering from Shenyang Agricultural University (SYAU), Shenyang, China, in 2017. He is currently working toward the M.Eng. degree in electrical engineering at the Southwest Jiaotong University (SWJTU), Chengdu, China.

His research interest is the thermal evaluation and condition monitoring of semiconductor devices in power electronic system.

Xinglai Ge (M'15) received the B.S., M.S., and Ph.D. degrees in electrical engineering from Southwest Jiaotong University (SWJTU), Chengdu, China, in 2001, 2004, and 2010, respectively. He is currently a Full Professor in the School of Electrical Engineering, Southwest Jiaotong University and a Vice Director of Department of Power Electronics and Power Drive.

From July to August of 2012, he was a visiting scholar at George Mason University, VA, USA. From October 2013 to October 2014, he was a visiting scholar at the School of Electrical and Computer Engineering, Georgia Institute of Technology, Atlanta, GA, USA. He is the author and co-author of more than 60 technical papers

His research interests include stability analysis and control of electrical traction system, fault diagnosis and hardware-in-the-loop simulation of traction converter and motor drive system.

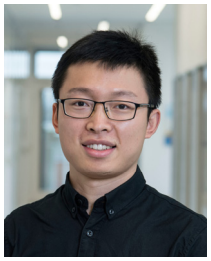

Yi Zhang (S'17-M20) received the B.S. and M.S. degrees in electrical engineering from Harbin Institute of Technology, Harbin, China, in 2014 and 2016, respectively, and the Ph.D. degree in power electronics from Aalborg University, Denmark. He is currently a Postdoctoral Fellow with Aalborg University, Denmark. He was a visiting scholar with Georgia Institute of Technology, USA from Nov. 2018 to Feb. 2019.

Dr. Zhang received the IEEE Power Electronics Society Ph.D. Thesis Talk Award Winner in 2020. He is the recipient of a research grant from the Danish Council for Independent Research (DFF-International Postdoc) affiliated with the Massachusetts Institute of Technology (MIT), USA in 2021.

Dong Xie (S'17) received the B.S. degree in electrical engineering from Southwest Jiaotong University, Chengdu, China, in 2017. He is currently working toward the Ph.D. degree in electrical engineering with the School of Electrical Engineering, Southwest Jiaotong University, Chengdu, China.

His research interests include fault diagnosis and fault-tolerant control of power electronic traction transformers for the traction system.

Mr. Xie was a recipient of the Best Paper Award of the International Conference on Electrical Machines and Systems (ICEMS) in 2019.

Bo Yao (S'17) received the B.Eng. degree and M.Eng. degree in electrical engineering from Southwest Jiaotong University (SWJTU), Chengdu, China, in 2017 and 2020, respectively. He is currently pursuing the PHD degree with power electronic in Aalborg University, Aalborg, Denmark.

His research interest is the reliability evaluation and condition monitoring of power electronic devices in power converter systems.

Mr. Yao was a recipient of the Best Paper Award of International Conference on Electrical Machines and Systems (ICEMS) in 2019.

Huimin Wang (S'17) received the B.Eng. degrees in electrical engineering from Southwest Jiaotong University (SWJTU), Chengdu, China, in 2016. He is currently working toward the Ph.D. degree in electrical engineering at the Southwest Jiaotong University, Chengdu, China.

His research interests include linear induction motor drive system and its speed-sensorless control.

Mr. Wang was a recipient of the Best Paper Award of IEEE Transportation Electrification Conference and EXPO Asia-Pacific (ITEC Asia-Pacific) in 2019.